CAUSALITY OF CIRCUIT AND ELECTROMAGNETIC-FIELD MODELS

Đorđević, A.R. Tošić, D.V. Sch. of Electr. Eng., Univ. of Belgrade, Belgrade, Serbia

Causality of Circuit and Electromagnetic-Field Models

Antonije R. Đorđević and Dejan V. Tošić

Abstract—**In the frequency-domain modeling of physical systems, such as electric circuits and electromagnetic-field structures, the problem of maintaining the causality of the time-domain response is an important issue in many engineering applications. The aim of the paper is to revisit some models for media parameters, transmission lines, and circuits.**

Index Terms—**Causality, Time-domain response**

I. INTRODUCTION

DESIGN of fast digital-signal interconnects is based on computer simulations (numerical modeling) of electromagnetic (EM) fields. These interconnects are vital parts of computers and communications equipment, and they are present both on integrated circuits and on printed-circuit boards (PCBs). Precise evaluation of timing and signal distortion requires accurate models of materials (dielectrics and conductors) on which the interconnects are built [1], [2]. Very wide signal bandwidths, extending into the millimeter-wave region, require characterization of materials in a wide frequency range. These models should accurately predict losses and provide causal responses in the time domain. Such models are also required for microwave circuits and devices, antennas, and other structures whose design is based on the EM simulations [3].

Recently, vendors of software systems for CAD/CAM of communication circuits have focused on resolving causality issues and implementing causal models in software tools [4]-[8]. They recognized the imperative need for major revision of traditional device and material models to fulfill the aforementioned causality in multilayer substrate models, loss models for composite dielectrics, device models, PCB models, and similar. For example, the goal in the selection of a dielectric model is to capture the physics of the material and to describe its complex dielectric constant as a continuous function of frequency, which guarantees a causal response, and not by just a set of points measured at various frequencies [9].

It is interesting to mention that even models of some well-known materials/substrates, such as FR-4, had to be amended. FR-4 has been in use since the 1960's (starting with TTL circuits). However, FR-4 printed-circuit boards have remained the technology of choice for low-cost

commercial digital and analog devices, and will likely prevail in the future as well.

In this paper, we consider causality issues for the modeling of circuits and EM structures, which belong to the class of linear, time-invariant, stable, and physically realizable systems. Examples are electrical circuits assembled from lumped elements (resistors, inductors, capacitors, etc.), RF/microwave filters, structures composed of (multiconductor) transmission-lines, antennas, and antenna arrays.

We assume that the system under consideration is void of accumulated electromagnetic energy for $t < 0$, where t is time. We also assume that the system is driven by one or more generators, which represent the excitation to the system. All these excitations are assumed zero for $t < 0$. One or more excitations "wake up" at $t = 0$. We are interested in the response of the system, which can be voltages, currents, waves, etc. Under these conditions, all signals (EM fields, voltages, and currents) in the system are zero for $t < 0$, as no response can occur before the excitation. This is a physically obvious fact and is the statement of the causality principle [10], [11].

In many cases, the analysis of electrical circuits and EM-field structures is performed by using the Fourier transform or the Laplace transform to switch between the time domain and the domain of the complex frequency, $s = \sigma + j\omega$, where σ is the real, and ω is the imaginary part. The imaginary part is referred to as the angular frequency, $\omega = 2\pi f$ (in s^{-1}), where f is the frequency (in Hz). The rationale for using the frequency-domain analysis is the fact that the time-domain differential equations map into the frequency-domain algebraic equations (by the Fourier or Laplace transforms) which are easier to solve (the derivative with respect to time is mapped into a simple multiplication by s in the frequency domain). Thereafter, equations that describe the system are formulated and solved in the complex domain.

Electrical circuits are analyzed in the complex domain starting from Kirchhoff's current law and voltage law (KCL and KVL), as well as equations that relate voltages and currents for each element of the circuit. EM-field structures are analyzed starting from Maxwell's equations for the electric and magnetic fields, along with constitutive relations that describe the dielectric, magnetic, and conductive properties of the medium. For linear time-invariant systems, all these equations are linear in terms of the voltages, currents, and field vectors.

Once the analysis in the complex domain is completed, we

Authors are with the School of Electrical Engineering, University of Belgrade, P.O. Box 35-54, 11120 Belgrade, Serbia (phone: + 381 11 3218 329; e-mail: edjordja@etf.rs).

can switch back to the time domain using the inverse Fourier transform or the inverse Laplace transform, as appropriate. Often, the adopted frequency-domain model of the system might be adequate for computing the frequency characteristics, but inadequate for switching back to the time domain via the inverse Fourier or Laplace transform. In that case, we can obtain a non-causal response in the time domain.

Inadequacies in the complex-domain model can come from overly simplifying the model or neglecting some small terms that are crucial for providing a causal response.

These simplifications do not occur in the KCL, KVL, or Maxwell's equations, but rather in circuit-element equations (component characteristics) and equations describing media/materials (constitutive equations). In Sections II and III, we give two representative examples for models that may yield non-causal responses, along with techniques for overcoming the problems.

Most results of the analysis in the frequency domain are in the form of certain network functions and transfer functions of a system (input impedance, scattering parameters, etc.). Collectively, we shall refer to these functions as the system functions, and denote them by $H(s)$. For most EM-field problems, the system functions can be obtained only numerically, in the form of tabulated data, i.e., no closed-form solution is available. In rare cases, such as uniform plane waves, uniform transmission lines, and waveguides, analytic solutions are available, and the system functions have the form of exponential functions (which, essentially, describe wave propagation). These system functions can be converted into forms that contain trigonometric or hyperbolic functions.

On the contrary, for most circuit-theory problems, the system functions can be obtained in a closed form. In particular, for lumped-element circuits (e.g., passive circuits that consist only of resistors, capacitors, and inductors), the system functions are rational functions of s, i.e., ratios of two polynomials. Poles of the rational functions are points in the s-plane where the system function becomes infinite. The poles are zeros of the denominator. An additional pole (simple or multiple) can be at infinity if the degree of the numerator is larger than the degree of the denominator. Similarly, zeros of the system function are zeros of the polynomial in the numerator, and an additional zero (simple or multiple) can be at infinity if the degree of the denominator is larger than the degree of the numerator. The stability criteria require that the poles of the system function are in the left-hand half-plane of the complex frequency, and that poles on the imaginary axis are simple. A transfer function can have zeros in the right half-plane, but an input impedance or admittance cannot have zeros in the right half-plane. A system function that does not have zeros in the right half-plane and has only simple zeros on the imaginary axis is referred to as a minimal-phase function. [12]

A system function that yields a causal response has some special properties. In particular, on the imaginary axis, its real and imaginary parts are related by the Hilbert transform [11], [13]. For a minimal-phase function, on the imaginary axis, the Hilbert transform also relates the logarithm of the

magnitude and the argument, so that the argument can be uniquely reconstructed knowing the magnitude of the transfer function, and vice versa [14]. However, the conditions for the existence of the transforms in both directions are strict. In Section IV, we demonstrate that the argument of a rational system function is always uniquely determined by its magnitude, on the imaginary axis, even in cases when the inverse Hilbert transform does not exist.

II. Modeling of Dielectric Losses

We consider an EM-field problem in the frequency domain, assuming that the complex frequency s is on the imaginary axis. Generally, the problem is described by the system of four Maxwell's equations, along with three constitutive relations:

$$\text{curl } \mathbf{E} = -j\omega\mathbf{B} , \tag{1}$$

$$\text{curl } \mathbf{H} = \mathbf{J} + j\omega\mathbf{D} , \tag{2}$$

$$\text{div } \mathbf{D} = \rho , \tag{3}$$

$$\text{div } \mathbf{B} = 0 , \tag{4}$$

$$\mathbf{D} = \varepsilon\mathbf{E} , \tag{5}$$

$$\mathbf{B} = \mu\mathbf{H} , \tag{6}$$

$$\mathbf{J} = \sigma(\mathbf{E} + \mathbf{E}_i) , \tag{7}$$

where $\mathbf{E}$ is the electric-field intensity vector, $\mathbf{D}$ is the electric-induction vector, $\mathbf{B}$ is the magnetic-induction vector, $\mathbf{H}$ is the magnetic-field intensity vector, $\mathbf{J}$ is the electric-current density vector, $\mathbf{E}_i$ is the impressed electric field (which models the excitation to the system), ρ is the volume-charge density, ε is the permittivity, μ is the permeability, and σ is the conductivity of the material. The quantities $\mathbf{E}$, $\mathbf{D}$, $\mathbf{B}$, $\mathbf{H}$, $\mathbf{J}$, $\mathbf{E}_i$, and ρ are the complex-domain representatives of the corresponding time-domain sinusoidal quantities.

Maxwell's equations are linear in terms of the field vectors and they do not introduce any problem regarding the causality. In the simplest model of the constitutive equations, ε, μ, and σ are purely real quantities that do not depend on frequency. Hence, the vectors on the right and left-hand sides of equations (5)-(7) are always in phase, and the resulting time-domain solution is always causal.

To model polarization losses and magnetization losses (i.e., to model dispersive media), the permittivity and permeability are taken to be complex quantities. (The conductivity is always taken to be real.) The complex permittivity and permeability have (in most cases) positive real parts and negative imaginary parts, so that they are written in the form $\varepsilon = \varepsilon_0(\varepsilon'-j\varepsilon'')$ and $\mu = \mu_0(\mu'-j\mu'')$, respectively, where $\varepsilon_r = \varepsilon'-j\varepsilon''$ is the relative permittivity, and $\mu_r = \mu'-j\mu''$ is the relative permeability of the material. The associated loss tangents (i.e., the dissipation factors) are

defined as $\tan\delta_\varepsilon = \dfrac{\varepsilon''}{\varepsilon'}$ and $\tan\delta_\mu = \dfrac{\mu''}{\mu'}$. We shall consider here only the dielectric losses. The magnetic losses can be treated in a similar way.

To provide a causal response, the complex permittivity has to satisfy certain conditions. It can be regarded as a scalar system function, like any other circuit-theory network function. When the complex frequency is purely imaginary, i.e., when $s = j\omega$, the system function is referred to as the frequency response and is given in terms of its modulus (magnitude) and argument (phase) as

$$H(j\omega) = A(\omega)\exp(j\phi(\omega)), \tag{8}$$

where $A(\omega) = |H(j\omega)|$ and $\phi(\omega) = \arg(H(j\omega))$. Alternatively, the system function is represented in terms of its real part (P) and imaginary part (Q) as

$$H(j\omega) = P(\omega) + jQ(\omega). \tag{9}$$

We consider only real-life systems, i.e., models of physically realizable systems that are characterized only by real parameters in the time domain. For example, all circuit-element values are real (resistances, capacitances, and inductances). Consequently, the system function will have conjugate symmetry: $H(s^*) = H^*(s)$, $H(-j\omega) = H^*(j\omega)$. Hence, the modulus and the real part are even functions of frequency, and the argument and the imaginary part are odd functions of frequency.

The impulse response $h(t)$ of any physical system is causal and can be represented by $h(t) = u(t)h(t)$, where $u(t)$ is the unit step function. Applying the Fourier transform (FT) [15], $\mathrm{FT}(h(t)) = \mathrm{FT}(u(t)h(t))$, and using the property $H(j\omega) = \dfrac{1}{2\pi}U(j\omega) \otimes H(j\omega)$, where $\otimes$ represents the convolution operator, $H(j\omega) = \mathrm{FT}(h(t))$, and $U(j\omega) = \mathrm{FT}(u(t)) = \pi\delta(\omega) + \dfrac{1}{j\omega}$ is the Fourier transform of the unit step function, we obtain $H(j\omega) = \dfrac{1}{2\pi}\int_{-\infty}^{\infty}(\pi\delta(\omega-\mu) + \dfrac{1}{j(\omega-\mu)})H(j\mu)\,d\mu$, which yields $H(j\omega) = \dfrac{1}{2}H(j\omega) + \dfrac{1}{2\pi j}\int_{-\infty}^{\infty}\dfrac{H(j\mu)}{\omega-\mu}\,d\mu$. Hence, the well-known relations between the real and imaginary parts of the frequency response follow:

$$P(\omega) = \frac{-1}{\pi}\,\text{v.p.}\int_{-\infty}^{\infty}\frac{Q(\mu)}{\mu-\omega}\,d\mu, \tag{10}$$

$$Q(\omega) = \frac{1}{\pi}\,\text{v.p.}\int_{-\infty}^{\infty}\frac{P(\mu)}{\mu-\omega}\,d\mu. \tag{11}$$

Both integrals are evaluated in the principal-value sense. It is assumed that the system function satisfies certain conditions that provide the existence of the two integrals. A sufficient condition is that the integrand is square-integrable along the imaginary axis.

From (10) and (11), knowing the real part of the frequency response, one can find the imaginary part, and vice versa. In practical computations, difficulties are often present due to the infinite limits of the integrals. A very wide spectrum must usually be encompassed to obtain a sufficiently accurate result. Even analytically, the integrals cannot be evaluated in many important practical cases because the integrals are divergent or undefined.

Noting that the real part is an even function, and the imaginary part is an odd function of frequency, equations (10) and (11) can be transformed to integrals over the real frequencies, $\omega > 0$:

$$P(\omega) = \frac{-2}{\pi}\,\text{v.p.}\int_{0}^{\infty}\frac{\mu Q(\mu)}{\mu^2-\omega^2}\,d\mu, \tag{12}$$

$$Q(\omega) = \frac{2\omega}{\pi}\,\text{v.p.}\int_{0}^{\infty}\frac{P(\mu)}{\mu^2-\omega^2}\,d\mu. \tag{13}$$

Relations (10)-(13) are commonly referred to as the Hilbert transforms (e.g., in electrical engineering, signal processing, and system theory) [16] or the Kramers-Kronig relations (e.g., in physics and material science) [17], [18]. Other forms of (similar) relations can be found in literature, e.g., [10], [14].

Derivation of (10)-(11) can be approached in a different way by using Cauchy's integral formula [19]. This approach yields more general relations, as will be shown in Section IV, and provides a better understanding of its limitations and the conditions for the frequency response. For example, $H(s)$ must be analytic in the right half of the s-plane, inclusive of the imaginary-axis, and $|H(s)|$ must not be an asymptotically increasing function when s tends to infinity [14], [16].

Often, for good dielectrics, the conductive losses are included into the permittivity, resulting in the equivalent permittivity, $\varepsilon_e = \varepsilon - j\dfrac{\sigma}{\omega}$. This modifies only the imaginary part of the permittivity. If the polarization losses are negligibly small (and thus ε is practically independent of frequency), then $\tan\delta_\varepsilon$ is proportional to $1/f$. The mathematical model of ε can be visualized as taking a parallel combination of a capacitor (whose capacitance is C) and a resistor (whose conductance is G), with frequency-independent parameters C and G. This maps into a standard circuit-theory problem and a causal response is naturally guaranteed. N ote that the real and imaginary parts of $\varepsilon_e(\omega)$ function cannot be shown to satisfy equations (10)-(13). The result of the integral in (10) is zero and so is the result of the integral in (11) if the principal-value sense is extended to the two infinite limits of the integral.

Physical mechanisms that cause polarization and magnetization losses are such that the parameters ε and μ, as well as the loss tangents, depend on frequency. For example, for high-quality dielectrics (like Teflon and polyethylene), $\tan\delta_\varepsilon$ increases practically linearly with frequency in the microwave region. However, if an overly simplified model

of the frequency dependence is taken, this can result in a non-causal response. For the present example, if we take ε' to be independent of frequency, and take only ε'' to vary linearly with frequency, we shall almost perfectly model the frequency dependence of $\tan\delta_\varepsilon$, but the time-domain response will not be causal. In other words, it is not possible to define independently the frequency variations of ε' and ε'' because these two quantities must be related by the Hilbert transform (provided the transform is convergent).

One approach to obtain a causal model is to select ε'' so to fit experimental data, and then evaluate ε' using the Hilbert transform. In the general case, this is not an easy task. Another way to obtain a causal model is to use functions that directly approximate $\varepsilon_r(\omega)$, for which we know *a priory* to yield a causal response. To approximate the linear frequency dependence of $\tan\delta_\varepsilon$, a simple choice is the one-pole function

$$\varepsilon_r(\omega) = \varepsilon'_\infty + \frac{\Delta\varepsilon'}{1 + j\dfrac{\omega}{\omega_0}} , \qquad (14)$$

where ε'_∞, $\Delta\varepsilon'$, and ω_0 are constants. We apply (14) when $\omega \ll \omega_0$, so that

$$\varepsilon_r(\omega) \approx \varepsilon'_\infty + \Delta\varepsilon'\left(1 - j\frac{\omega}{\omega_0}\right) = (\varepsilon'_\infty + \Delta\varepsilon') - j\frac{\Delta\varepsilon'\omega}{\omega_0} , \qquad (15)$$

$$\tan\delta_\varepsilon(\omega) \approx \frac{\Delta\varepsilon'\omega}{\omega_0(\varepsilon'_\infty + \Delta\varepsilon')} . \qquad (16)$$

Hence, if we know the relative permittivity at low frequencies, $\varepsilon'(0) = (\varepsilon'_\infty + \Delta\varepsilon')$, and the loss tangent at a particular frequency ($f = 10$ GHz is standard for microwaves), then we can adopt ω_0 arbitrarily (but so to be high above the frequency band of interest) and calculate the remaining two parameters accordingly. This model yields a causal response as it corresponds to the simple network shown in Fig. 1, where $\omega_0 R_1 C_1 = 1$.
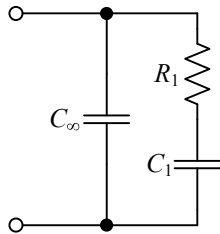

Fig. 1. Simple electric network that corresponds to equation (14).

Another important example is the material FR-4, often used as the substrate for fabrication of printed-circuit boards. In a very wide frequency range, starting from the power frequencies, up into the microwave region, this material is known to have a loss tangent that is practically independent of frequency. The measured data for this material are shown in Fig. 2 [20].
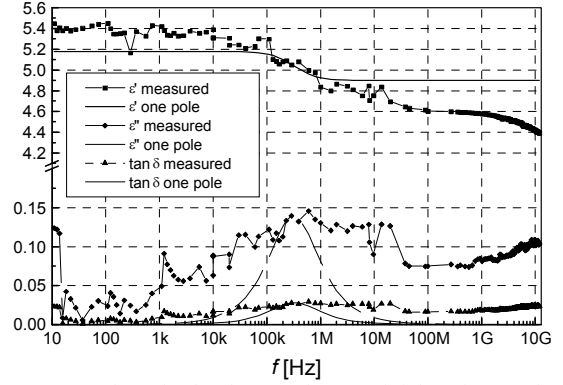

Fig. 2. Measured results for the complex permittivity of FR-4 along with one-pole model according to (14) [20].

The simplest model for this material is to take both ε' and ε'' to be independent of frequency. However, this results in a noncausal response, as illustrated by the following example. We consider a uniform plane EM wave that propagates through an infinite medium filled with FR-4. We excite a wave at the coordinate origin, whose time-domain waveform is a Dirac delta-function (an impulse), centered at $t = 0$. The wave propagates along a distance of 1 m, where we observe the response. From the physical nature of propagation, we would expect the wave to arrive with a delay on the order of several nanoseconds. However, if we take $\varepsilon' = 4.5$ and $\varepsilon'' = 0.1$ to be independent of frequency (corresponding to a frequency-independent loss tangent), describe the propagation by the exponential factor, and evaluate the time-domain response using the inverse fast Fourier transform (IFFT), the resulting waveform will not be causal, as shown in Fig. 3. The response does not have a defined starting instant, but it has rather a long, slowly increasing "foretail", which starts at $t = 0$.

We can try to model the relative permittivity of FR-4 by taking the approximation given by (14) and dragging ω_0 into the frequency band of interest (Fig. 2). This yields a causal response, but the approximation of losses is inadequate for broadband applications (such as analysis of transients in fast digital-signal interconnects) because it covers barely one frequency decade. Note from Fig. 2 that there is a step-down in ε' in the frequency band where ε'' is pronounced.
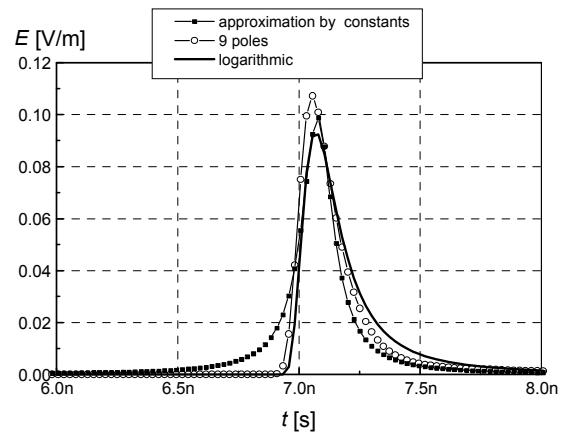

Fig. 3. Response to an impulse wave in FR-4 for various models of frequency variations of the permittivity [20].

To obtain an approximation for $\varepsilon_r(\omega)$ in a wider frequency range, more terms are required. This procedure corresponds to the network shown in Fig. 4 [20] and it results in

$$\varepsilon_r(\omega) = \varepsilon'_\infty + \sum_{i=1}^{N} \frac{\Delta\varepsilon'_i}{1 + j\dfrac{\omega}{\omega_i}} - j\frac{\sigma}{\omega\varepsilon_0} . \qquad (17)$$

The resistor R_0 models conductive losses (which are dominant at very low frequencies). For $N = 8$ (i.e., for a total of 9 poles), the coefficients that best fit the measured data are given in Table 1 [20]. The relative permittivity that corresponds to this approximation is shown in Fig. 5. The time-domain response is now causal, as shown in Fig. 3.
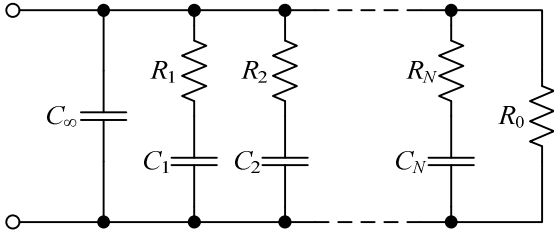

Fig. 4. Electric network that corresponds to equation (17) [20].

TABLE 1. COEFFICIENTS IN EQUATION (17) THAT FIT MEASURED DATA FOR FR-4 IN A BROAD FREQUENCY RANGE.

i	1	2	3	4	5	6	7	8
$\omega_i \ [\mathrm{s}^{-1}]$	20k	0.2M	2M	20M	0.2G	2G	20G	0.2T
$\Delta\varepsilon'_i$	0.12	0.14	0.22	0.18	0.12	0.10	0.10	0.24

In Table 1, the fitting terms are taken one per frequency decade. A finer approximation can be obtained if we increase the density of the fitting terms.

If we distribute the terms evenly on a logarithmic-frequency scale, if we assume ε'' to be constant in the frequency range from $\omega_1 = 10^{m_1}$ up to $\omega_2 = 10^{m_2}$, and if the total variation of ε' in this range is $\Delta\varepsilon'$ (i.e., the variation slope is $\dfrac{\Delta\varepsilon'}{m_2 - m_1}$ per decade), we obtain in the limit when $N \to +\infty$

$$\sum_{i=1}^{N} \frac{\Delta\varepsilon'_i}{1 + j\dfrac{\omega}{\omega_i}} \to \frac{\Delta\varepsilon'}{m_2 - m_1} \int_{x=m_1}^{m_2} \frac{\mathrm{d}x}{1 + j\dfrac{\omega}{10^x}} = \frac{\Delta\varepsilon'}{m_2 - m_1} \frac{\ln\dfrac{\omega_2 + j\omega}{\omega_1 + j\omega}}{\ln 10} . \qquad (18)$$

The complex relative permittivity now becomes

$$\varepsilon_r(\omega) = \varepsilon'_\infty + \frac{\Delta\varepsilon'}{m_2 - m_1} \frac{\ln\dfrac{\omega_2 + j\omega}{\omega_1 + j\omega}}{\ln 10} - j\frac{\sigma}{\omega\varepsilon_o} . \qquad (19)$$

In the frequency range where $\omega_1 \ll \omega \ll \omega_2$, the real part of the integral in (18) is

$$\mathrm{Re}\left\{ \frac{\Delta\varepsilon'}{m_2 - m_1} \frac{\ln\dfrac{\omega_2 + j\omega}{\omega_1 + j\omega}}{\ln 10} \right\} = \frac{\Delta\varepsilon'}{m_2 - m_1} \frac{\ln\left|\dfrac{\omega_2 + j\omega}{\omega_1 + j\omega}\right|}{\ln 10}$$

$$\approx \frac{\Delta\varepsilon'}{m_2 - m_1} \frac{\ln\dfrac{\omega_2}{\omega}}{\ln 10} . \qquad (20)$$

It linearly decays with the logarithm of frequency. The imaginary part is practically independent of frequency,

$$\mathrm{Im}\left\{ \frac{\Delta\varepsilon'}{m_2 - m_1} \frac{\ln\dfrac{\omega_2 + j\omega}{\omega_1 + j\omega}}{\ln 10} \right\} = \frac{\Delta\varepsilon'}{m_2 - m_1} \frac{\arg\left\{\dfrac{\omega_2 + j\omega}{\omega_1 + j\omega}\right\}}{\ln 10}$$

$$\approx \frac{\Delta\varepsilon'}{m_2 - m_1} \frac{-\dfrac{\pi}{2}}{\ln 10} . \qquad (21)$$

Fig. 5 demonstrates how the approximation (19) fits the measured data. The corresponding time-domain response is causal, as shown in Fig. 3.
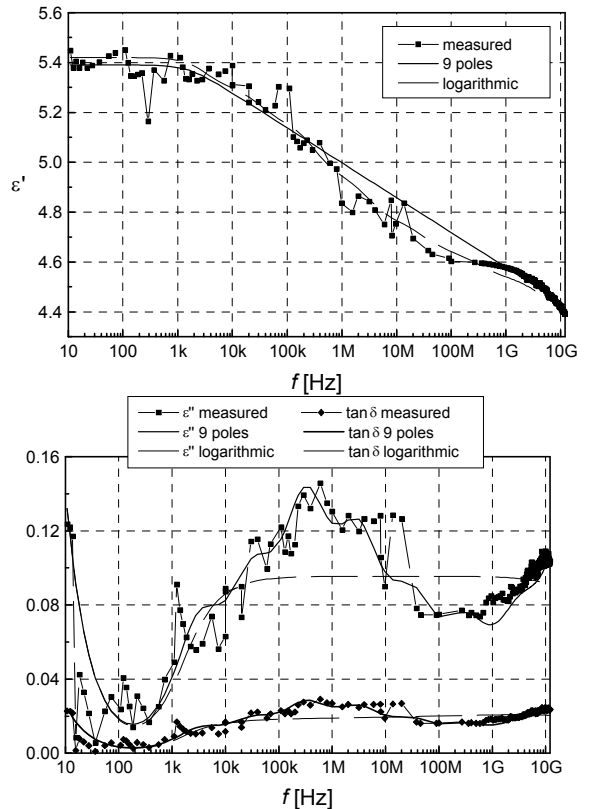

Fig. 5. Fitting measured data by equations (17) and (19) [20].

As digital systems evolve and technology pushes for smaller and faster designs, higher data transmission rates necessitate the use of proper techniques to model the frequency dependent parameters of materials, such as FR-4. Without proper models that accurately predict these quantities and that are required to preserve causality, simulation-based design, such as bus design for multi-gigabit

data rates, is not possible. For that reason, the model described by equation (19) has recently found application in the research and development, as well as in leading software for the analysis of fast digital-signal interconnects [1], [2], [4]-[9], [21]-[24].
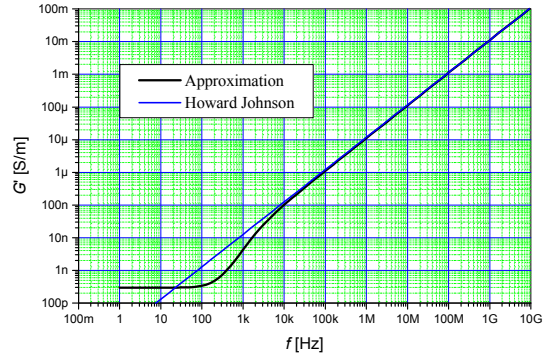
III. TRANSMISSION-LINE MODELS

One practical problem that relies on the adequate modeling of the dielectric permittivity is signal propagation along transmission lines. A simple line (with two signal conductors) can be characterized with sufficient accuracy [25] by its primary quasi-static per-unit-length parameters: inductance (L'), capacitance (C'), resistance (R'), and conductance (G').This approach yields better models than using just the characteristic impedance, attenuation coefficient, and phase coefficient, in particular for shorter lines [26]. We neglect here the hybrid nature of the quasi-TEM waves and the corresponding variations of the field pattern.

In practice, transmission lines are lossy and their primary parameters depend on frequency. For example, if the dielectric is homogeneous, the per-unit-length admittance matrix of the line can be put in the form $Y' = G' + j\omega C' = j\omega C_0'(\varepsilon' - j\varepsilon'')$, where C_0' is the per-unit-length capacitance of the line when the dielectric is replaced by a vacuum, and $\varepsilon_r = \varepsilon' - j\varepsilon''$ is the complex relative permittivity of the dielectric. As discusses in Section II, for a realistic lossy dielectric, ε' and ε'' are frequency-dependent. Hence, the frequency variations of C' and G' are determined by $\varepsilon'(\omega)$ and $\omega\varepsilon''(\omega)$, respectively. An example of these primary parameters is shown in Fig. 6 (the curve labeled "Approximation"), corresponding to a router backplane on FR-4. If we obey the causality constraints discussed in Section II, we shall provide a proper model for Y', which will provide a causal response. For lines with inhomogeneous dielectrics, the procedure described in [20] can be used, where the frequency variations of Y' are approximated by a linearization technique.

In [27], a causal model of the relative permittivity with a constant loss tangent is given: $\varepsilon_r = a\,(j\omega)^{-2\delta/\pi}$, where a is a constant. This model agrees perfectly with (19) when $\omega_1 \ll \omega \ll \omega_2$. However, this model yields unnatural results in limiting cases: an infinite permittivity when $\omega \to 0$ (Fig. 6, the curve labeled "Howard Johnson") and a vanishing permittivity when $\omega \to \infty$.

The frequency dependence of the per-unit-length impedance, $Z' = R' + j\omega L'$, is more complicated in nature [28], [29] because it is affected by the edge, proximity, and skin effects. If we consider a printed structure, like a microstrip line, at lower frequencies, the current distribution exhibits significant variations along the width of the strip and the ground plane, and then the skin effect occurs. At very high frequencies, typically above about 1 GHz, the surface roughness of the conductors becomes pronounced.

(a)
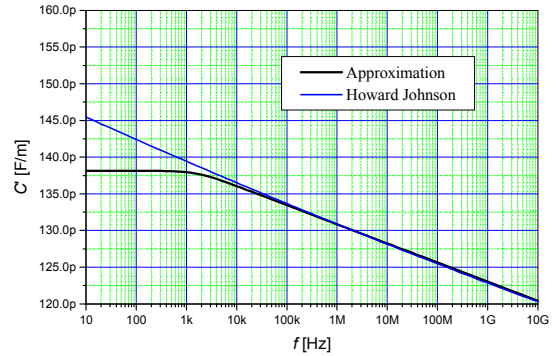
(b)

Fig. 6. Per-unit-length (a) conductance and (b) capacitance of a transmission line using the lossy-dielectric model of equation (19) and [27].

If the frequency variations of R' and L' are modeled independently, like in [28], a noncausal response results. In order to properly model the frequency dependence of Z', a similar approach should be used as presented in Section II, that is to describe Z' by an analytic function of the complex frequency.

A model is presented in [30] for the differential-mode propagation on coupled striplines:

$$Z' = R'_{\text{d.c.}} + j\omega L'_\infty + R'_{\text{ref}} \sqrt{\frac{2j\omega}{\omega_{\text{ref}}} \frac{\dfrac{j\omega}{\omega_{\text{skin}}}}{1 + \dfrac{j\omega}{\omega_{\text{skin}}}}} \frac{1 + 2\sqrt{\dfrac{j\omega}{\omega_{\text{rgh}}}}}{1 + \sqrt{\dfrac{j\omega}{\omega_{\text{rgh}}}}}, \quad (22)$$

where L'_∞ is the per-unit-length external inductance (as evaluated, for example, by [25]). Other parameters are evaluated based on theoretical estimations and data fitting for the particular transmission line under consideration: $f_{\text{skin}} = 19\,\text{MHz}$ is the frequency where the skin-effect becomes pronounced, whereas the surface roughness becomes visible at $f_{\text{rgh}} = 600\,\text{MHz}$. In [27], another model is given,

$$Z' = j\omega L'_\infty + \sqrt{R'^2_{\text{d.c.}} + \frac{2j\omega}{\omega_{\text{ref}}} R'^2_{\text{ref}}}. \quad (23)$$

Fig. 7 shows the per-unit-length resistance and inductance, versus frequency, obtained by various techniques. The curves labeled "Approximation" correspond to equation (22), and those labeled "Howard Johnson" correspond to (23). The curves labeled "No surface roughness" are evaluated from (22) assuming $\omega_{skin} \to +\infty$. The curves labeled "Skin effect" are evaluated by program [25], which assumes the skin effect to be fully pronounced at all frequencies. The resistance given by the curve labeled "Surface roughness" in Fig. 7a is two times the resistance given by [25] and it represents the upper limit of the resistance increased due to the surface roughness. In Fig. 7a, "D.C." is the d.c. resistance. The curves labeled "TM dynamic" are obtained by a full-wave analysis described in [29], and the curves labeled "Quasistatic" by a quasistatic technique from [29]. Obviously, the d.c. behavior is not accurately described by either equation (22) or (23), so that further investigation of this topic is needed.
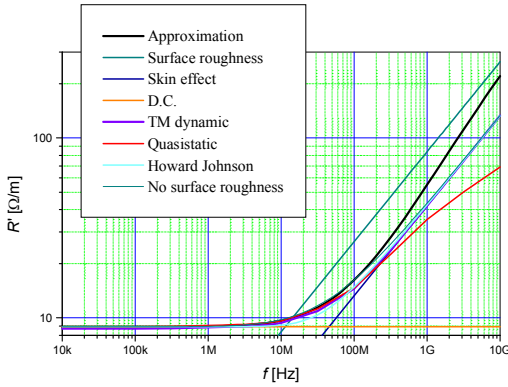
(a)
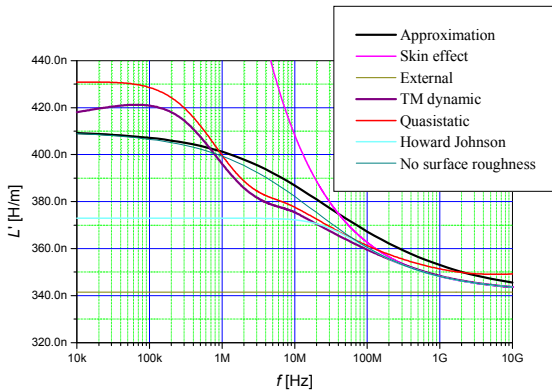
(b)

Fig. 7. Per-unit-length (a) resistance and (b) inductance of a transmission line obtained using various techniques.

IV. CAUSALITY AND HILBERT TRANSFORM

We consider an analytic function that does not have poles in the right half-plane or on the imaginary axis, i.e., which is a strictly stable function[1]. Its modulus, argument, real part, and imaginary part are defined in equations (8) and (9).

---

[1] It need not be a minimal-phase function.

Using the contour integration, it is shown in [14], [13] that the real and imaginary parts of such a function satisfy the following relations:

$$P(\omega) = P(\infty) - \frac{1}{\pi} \, \text{v.p.} \int_{-\infty}^{\infty} \frac{Q(\mu)}{\mu - \omega} \, d\mu, \qquad (24)$$

$$Q(\omega) = \frac{1}{\pi} \, \text{v.p.} \int_{-\infty}^{\infty} \frac{P(\mu)}{\mu - \omega} \, d\mu. \qquad (25)$$

The assumption is that the function $H(s)$ is finite at infinity. More precisely, it is constant and equal to $P(\infty)$, where $P(\infty)$ can be any real number. Obviously, any analytic function that satisfies these conditions can be a system function that yields a causal response. The additive constant does not affect the causality and it can be set to zero, in which case we obtain relations (10) and (11).

The set of relations (24) and (25) is of restrictive validity. The functions $P(\omega)$ and $Q(\omega)$ must be such that the integrals exist in the principal-value sense. Many common functions found in the circuit theory cannot fit into these equations. For example, a unit ideal differentiator (e.g., the input impedance of an ideal coil of a unit inductance), whose frequency response has the form $H(j\omega) = j\omega$, does not belong to the above class of functions as it has a pole at infinity. The reciprocal function, $H(j\omega) = \frac{1}{j\omega}$, i.e., a unit ideal integrator, also cannot fit into the Hilbert transform as it has a pole at the coordinate origin (which is on the imaginary axis).

We consider a strictly stable system function, $H(s)$, which yields a causal response. Taking the logarithm of the frequency response results in

$$\ln H(j\omega) = \ln |H(j\omega)| + j \arg(H(j\omega)) = a(\omega) + j\phi(\omega). \quad (26)$$

The real part, $a(\omega) = \ln |H(j\omega)| = \ln A(\omega)$, is the logarithmic modulus of the frequency response (in nepers). The imaginary part, $\phi(\omega)$, is the argument (in radians) of $H(j\omega)$. Taking a logarithm is a nonlinear operation. Hence, there is no reason following from the causality why there should be any relation between $a(\omega)$ and $\phi(\omega)$ in the general case. However, equations (24) and (25) relate the real and imaginary part of any analytic function that satisfies the above-mentioned conditions [14], [31]. A strictly stable system function, $H(s)$, has no poles in the right half-plane nor on the imaginary axis. If, in addition, it has no zeros in the right half-plane or on the imaginary axis (i.e., it is a strictly minimal-phase function), then $\ln H(s)$ is finite in the right half-plane and on the imaginary axis, i.e., it has no poles there. To make $\ln H(s)$ finite at infinity, $H(s)$ must tend to a non-zero constant when $s \to \infty$. If all these conditions are met, then $a(\omega)$ and $\phi(\omega)$ are related as

$$a(\omega) = a(\infty) - \frac{1}{\pi} \, \text{v.p.} \int_{-\infty}^{\infty} \frac{\phi(\mu)}{\mu - \omega} \, d\mu, \qquad (27)$$

$$\phi(\omega) = \frac{1}{\pi} \text{ v.p.} \int_{-\infty}^{\infty} \frac{a(\mu)}{\mu - \omega} \, d\mu . \tag{28}$$

Hence, under the above restrictions, knowing the logarithmic magnitude of the frequency response, the corresponding argument is uniquely defined by the Hilbert transform, and vice versa [32].

We prove here that the argument of a stable rational minimal-phase system function is uniquely defined by its magnitude, on the imaginary axis, under more relaxed conditions, though the reverse relation may not exist in all cases. We factor the rational system function as

$$H(s) = \frac{M(s)}{N(s)} = k \frac{\prod_{i=1}^{m}(s - s_i)}{\prod_{j=1}^{n}(s - s_j)}, \tag{29}$$

where k is a constant, $M(s)$ is the polynomial in the numerator whose order is m, $N(s)$ is the polynomial in the denominator whose order is n; s_i is a zero of the numerator (which is also a zero of the system function), and s_j is a zero of the denominator (which is also a pole of the system function). The stability criteria require that the poles be only in the left-hand plane. If they are on the imaginary axis, they must be simple. From the assumption that we consider a minimal-phase rational function, the zeros are also only in the left half-plane or on the imaginary axis. Poles and zeros appear in conjugate symmetry: for each zero (or pole) that is not on the real axis, there exists a corresponding conjugate-complex zero (or pole), i.e., they always appear in pairs $s_{1,2} = \sigma_1 \pm j\omega_1$.

Since $a(\omega)$ is an even function of frequency, the Hilbert transform of this function can be written as

$$\phi(\omega) = \frac{1}{\pi} \text{ v.p.} \int_{-\infty}^{\infty} \frac{a(\mu)}{\mu - \omega} \, d\mu = \frac{2\omega}{\pi} \text{ v.p.} \int_{0}^{\infty} \frac{a(\mu)}{\mu^2 - \omega^2} \, d\mu . \tag{30}$$

Similarly, $\phi(\omega)$ is an odd function of frequency, so that the Hilbert transform can be written as

$$a(\omega) = \frac{-1}{\pi} \text{ v.p.} \int_{-\infty}^{\infty} \frac{\phi(\mu)}{\mu - \omega} \, d\mu = \frac{-2}{\pi} \text{ v.p.} \int_{0}^{\infty} \frac{\mu\phi(\mu)}{\mu^2 - \omega^2} \, d\mu . \tag{31}$$

Equations (30) and (31) are Kramers-Kronig relations.
From [33] (formula 4.231.10) we have

$$\int_{0}^{+\infty} \frac{\ln x}{a^2 - b^2 x^2} \, dx = -\frac{\pi^2}{4ab} , \quad ab > 0 . \tag{32}$$

For $a = y$ and $b = 1$, we have

$$\int_{0}^{+\infty} \frac{\ln x}{y^2 - x^2} \, dx = -\frac{\pi^2}{4y} , \quad y > 0 , \tag{33}$$

so that

$$\frac{1}{\pi} \text{ v.p.} \int_{-\infty}^{+\infty} \frac{\ln |\mu|}{\mu - \omega} \, d\mu = \frac{\pi}{2} \text{ sign } \omega \tag{34}$$

because the Hilbert transform of an even function is an odd function, and vice versa.
From [33] (formula 4.295.8) we have

$$\int_{0}^{+\infty} \frac{\ln(a^2 + b^2 x^2)}{c^2 - g^2 x^2} \, dx = -\frac{\pi}{cg} \text{ arctg } \frac{bc}{ag} , \quad a,b,c,g > 0 . \tag{35}$$

For $b = 1$, $c = y$, and $g = 1$, we have

$$\int_{0}^{+\infty} \frac{\ln(a^2 + x^2)}{y^2 - x^2} \, dx = -\frac{\pi}{y} \text{ arctg } \frac{y}{a} , \quad y > 0 . \tag{36}$$

Hence,

$$\frac{1}{\pi} \text{ v.p.} \int_{-\infty}^{+\infty} \frac{\frac{1}{2}\ln(a^2 + \mu^2)}{\mu - \omega} \, d\mu = \text{arctg } \frac{\omega}{a} . \tag{37}$$

When the complex frequency is on the imaginary axis ($s = j\omega$), all factors (binomials) of the system function have the form $j\omega - s_1 = -\sigma_1 + j(\omega - \omega_1)$, where $\sigma_1 \leq 0$. The logarithmic modulus of such a term has the form

$$a_1(\omega) = \ln | j\omega - s_1 | = \frac{1}{2}\ln\left(\sigma_1^2 + (\omega - \omega_1)^2\right), \tag{38}$$

and the argument is

$$\phi_1(\omega) = \arg(j\omega - s_1) = \text{arctg } \frac{\omega - \omega_1}{-\sigma_1} . \tag{39}$$

In the simplest case when the zero of the polynomial is at the coordinate origin ($s_1 = 0$), the factor is merely $j\omega$, so that $a_1(\omega) = \ln |\omega|$ and $\phi_1(\omega) = \frac{\pi}{2} \text{sign } \omega$. This is in accordance with (34): the argument is indeed obtained by applying the Hilbert transform to the logarithmic modulus. In other words, the argument can be reconstructed from the magnitude. The inverse relation does not exist because the integral

$$a(\omega) = -\frac{1}{\pi} \text{ v.p.} \int_{-\infty}^{\infty} \frac{\frac{\pi}{2}\text{sign } \mu}{\mu - \omega} \, d\mu = - \text{ v.p.} \int_{0}^{\infty} \frac{\mu}{\mu^2 - \omega^2} \, d\mu \tag{40}$$

diverges. Hence, knowing an argument that has the form $\phi_1(\omega) = \text{arctg } \frac{\omega - \omega_1}{-\sigma_1}$, the magnitude cannot be calculated using the Hilbert transform.

When the polynomial zero is on the imaginary axis ($s_1 = j\omega_1$), then $a_1(\omega) = \ln |\omega - \omega_1|$ and $\phi_1(\omega) = \frac{\pi}{2} \text{sign } (\omega - \omega_1)$, which is a simple translation of the previous case along the imaginary axis. Now,

$$\frac{1}{\pi} \text{ v.p.} \int\limits_{-\infty}^{+\infty} \frac{\ln|\mu - \omega_1|}{\mu - \omega} d\mu = \frac{1}{\pi} \text{ v.p.} \int\limits_{-\infty}^{+\infty} \frac{\ln|\mu'|}{\mu' + \omega_1 - \omega} d\mu'$$

$$= \frac{\pi}{2} \text{sign}(\omega - \omega_1). \tag{41}$$

Again, the argument can be uniquely reconstructed from the magnitude of this term.

When the polynomial zero is on the negative part of the real axis ($s_1 = \sigma_1 < 0$), then

$$a_1(\omega) = \ln\sqrt{\sigma_1^2 + \omega^2} = \frac{1}{2}\ln(\sigma_1^2 + \omega^2) \quad \text{and}$$

$\phi_1(\omega) = \text{arctg}\, \dfrac{\omega}{-\sigma_1}$. From (36) it follows that

$$\frac{1}{\pi} \text{ v.p.} \int\limits_{-\infty}^{+\infty} \frac{\frac{1}{2}\ln(\mu^2 + \sigma_1^2)}{\mu - \omega} d\mu = \text{arctg}\, \frac{\omega}{-\sigma_1} \tag{42}$$

(because $\sqrt{\sigma_1^2} = |\sigma_1| = -\sigma_1$). In trying to derive the inverse relation, an infinite integral is obtained, so that the magnitude cannot be calculated from the argument.

Finally, if the polynomial zero is at an arbitrary location in the left half-plane ($s_1 = \sigma_1 + j\omega_1, \sigma_1 < 0$), then

$$a_1(\omega) = \frac{1}{2}\ln\!\left(\sigma_1^2 + (\omega - \omega_1)^2\right) = \ln\sqrt{\sigma_1^2 + (\omega - \omega_1)^2} \quad \text{and}$$

$\phi_1(\omega) = \text{arctg}\, \dfrac{\omega - \omega_1}{-\sigma_1}$. The proof is derived from the previous case, by frequency translation, as already done for the zero on the imaginary axis.

If the above procedure is applied to each term of the factored fraction, after taking the logarithm, we obtain a sum of logarithms of the factors. The above relations are valid for each term of this sum. Hence, the argument of a stable minimal-phase rational function can be obtained as the Hilbert transform of the logarithmic modulus. This conclusion is valid for any rational system function under the condition that the function has no zeros or poles in the right half-plane. Stable minimal-phase rational functions are a subset of such functions. A unit ideal differentiator and integrator also belong to the class of functions for which the argument can be evaluated from the magnitude, though the reverse operation is not defined.

There exist physically realizable functions for which the logarithmic magnitude and argument are not interrelated by the Hilbert transform, not even in one way. For example, an all-pass function (which can be a stand-alone function or appear as a product in a rational function of a non-minimal phase) has a constant (unit) magnitude on the imaginary axis. The logarithmic magnitude is zero, but the argument is nonzero (although a zero results from the Hilbert transform). This is not in contradiction with the above presentation for rational functions, as the all-pass function has zeros in the right half-plane. Hence, it does not satisfy conditions for the existence of the transforms in (24), (25), (27), and (28). Similarly, for a lossless transmission line, the transfer function on the imaginary axis has the form $\exp(-j\tau\omega)$,

where τ is a real constant ($\tau \geq 0$). The logarithmic magnitude is also zero, but the argument is a linear function of frequency. The transforms (24) and (25) are invalid in this case because the function $\exp(-\tau s)$ has a singularity at infinity.

V. Conclusion

Models of dielectric parameters are presented that yield a causal response in the time domain. The models are based on fitting experimental data by functions that automatically provide causality. Models are also presented for the primary parameters of transmission lines that guarantee causal response in the time domain.

Relations between the argument and modulus of input and transfer functions, on the imaginary axis, are revisited. General conditions for the validity of these relations are underlined. For the class of minimal-phase stable rational functions, it is shown that the phase response can be reconstructed from the magnitude response under substantially relaxed conditions than in the general case.

References

[1] S. H. Hall and H. L. Heck, *Advanced Signal Integrity for High-Speed Digital Designs*, John Wiley & Sons, Inc., Hoboken, NJ, 2009.

[2] H. Heck, "PCB modeling requirements for PC systems", *Intel Corporation*, http://www.intel.com/, April 12, 2010.

[3] N. Kinayman and M. I. Aksun, *Modern Microwave Circuits*, Artech House, Norwood, MA, 2005.

[4] J. DeLap, "3D simulations for signal integrity", *Ansoft*, http://www.ansoft.com/, 2008.

[5] Simbeor Application Note #2008_06, "Modeling frequency-dependent dielectric loss and dispersion for multi-gigabit data channels", *Simberian*, Inc., http://www.simberian.com/, Sept. 2008.

[6] Y. Shlepnev, A. Neves, T. Dagostino, S. McMorrow, "Measurement-assisted electromagnetic extraction of interconnect parameters on low-cost FR-4 boards for 6-20 Gb/sec applications", *DesignCon* 2009.

[7] Advanced Design System 2009, "The HF/Hi-speed co-design platform", *Agilent Technologies*, http://www.agilent.com/, 2009.

[8] D. Huang, "Advanced EDA tools to improve the high-speed PCB and connector design, *Agilent Technologies*, http://www.agilentads.com/, Feb. 2010.

[9] Y. Shlepnev, A. Neves, T. Dagostino, S. McMorrow, "Practical identification of dispersive dielectric models with generalized modal S-parameters for analysis of interconnects in 6-100 Gb/s applications", *DesignCon* 2010.

[10] H. W. Bode, *Network Analysis and Feedback Amplifier Design*, D. Van Nostrand Company, Inc., Princeton, New Jersey, 1945.

[11] I. S. Stojanović, *Fundamentals of Telecommunications*, BIGZ, Belgrade, Serbia, 1972.

[12] B. J. Leon, *Lumped Systems*, Holt, Rinehart and Winston, Inc., New York, NY, 1968.

[13] B. Raković, *Linear Integrated Circuits*, Mikro knjiga, Belgrade, Serbia, 1991.

[14] E. A. Guillemin, *Theory of Linear Physical Systems*, John Wiley & Sons, Inc., New York, NY, 1963.

[15] R. N. Bracewell, *The Fourier Transform and Its Applications*, 3rd Ed., McGraw-Hill, New York, NY, 2000.

[16] O. Wing, *Classical Circuit Theory*, Springer Science+Business Media, LLC, New York, NY, 2008.

[17] R. de L. Kronig, "On the theory of the dispersion of X-rays", *Journal of the Optical Society of America*, vol. 12, no. 6, pp. 547-557, 1926.

[18] H. A. Kramers, "La diffusion de la lumière par les atomes", Estratto dagli Atti del *Congresso Internazionale dei Fisíci*, Como, vol. 2, 1927, pp. 545-557.

[19] E. Freitag and R. Busam, *Complex Analysis*, 2nd Ed., Springer-Verlag, Berlin, Germany, 2009.

[20] A. R. Djordjević, R. M. Biljić, V. D. Likar-Smiljanić, T. K. Sarkar, "Wideband frequency-domain characterization of FR-4 and time-

domain causality", *IEEE Trans. Electromagn. Compat.*, vol. EMC-43, no. 4, pp. 662-667, Nov. 2001.

[21] S. Hall, T. Liang, H. Heck, and D. Shykind, "Modeling requirements for transmission lines in multi-gigabit systems," in *Electrical Performance of Electronic Packaging*, Portland, Oregon, Oct. 2004, pp. 67-70.

[22] J. R. Miller, G. Blando, and I. Novak, "Crosstalk due to periodic plane cutouts", *DesignCon* 2007.

[23] V. Zwillich, M. Wollitzer, T. Wirschem, W. Menzel, and H. Leier, "Signal integrity analysis of a 1.5 Gbit/s LVDS video Link", in *Proc. IEEE EMC Symposium* 2007.

[24] F. Rao and C. Morgan, "The need for impulse response models and an accurate method for impulse generation from band-limited S-parameters", *DesignCon* 2008.

[25] A.R. Djordjević, M.B. Baždar, R.F. Harrington, and T.K. Sarkar, *LINPAR for Windows: Matrix Parameters for Multiconductor Transmission Lines, Version 2.0.* Artech House, Boston, MA, 1999.

[26] A. R. Djordjević, A. G. Zajić, D. V. Tošić, and T. Hoang, "A Note on the Modeling of Transmission-Line Losses", *IEEE Trans. Microwave Theory Tech.*, vol. 51, no. 2, pp. 483-486, Feb. 2003.

[27] H. Johnson and M. Graham, *High-Speed Signal Propagation*, Prentice Hall, Upper Saddle River, NJ, 2003.

[28] A. R. Djordjević and T. K. Sarkar, "Closed-form formulas for frequency-dependent resistance and inductance per unit length of microstrip and strip transmission lines", *IEEE Trans. Microwave Theory Techn.*, vol. MTT-42, no. 2, Feb. 1994, pp. 241-248.

[29] T. K. Sarkar and A. R. Djordjević, "Wideband electromagnetic analysis of finite-conductivity cylinders", *Progress in Electromagnetic Research*, vol. 16, pp. 153-173, 1997.

[30] I. D. Jovanović, *Ultrafast Digital-Signal Interconnects on Printed-Circuit Boards*, M.Sc. Thesis, University of Belgrade, School of Electrical Engineering, 2010.

[31] R. E. A. C. Paley and N. Wiener, *Fourier Transforms in the Complex Domain*. American Mathematical Society Colloquium Publications, vol. 19, Ch. I, Quasi-analytic Functions, Theorem XII, pp. 16-17, 1934.

[32] A. R. Djordjević, "Causality of circuit and electromagnetic-field models", *CXXXII Bulletin of Serbian Academy of Sciences and Arts*, no. 30, pp. 33-59, 2006.

[33] И. С. Градштейн и И. М. Ръижик, *Таблици интегралов, сумм, ряадов и произведений*, Наука, Москва, 1971.